



# UNIVERSITY OF TWENTE.

Faculty of Engineering Technology -  
Biomechanical Engineering

## Analysis of IRONSperm using multi-flagellated propulsion

Tom L. Zwijnenberg  
B.Sc. Thesis  
September 2022

---

**Graduation committee members:**

Dr. I.S.M. Khalil  
Prof.Dr. S. Misra  
Prof. Dr. Ir. L. Abelman

**Report number:**

BE-890

Faculty of Engineering Technology,  
Biomechanical Engineering  
University of Twente

---



# Abstract

In this research we will look at the movement of biohybrid magnetic microrobots by electrostatic self-assembly of dead bovine sperm cells with the goal to achieve targeted drug delivery. The IRONSperms propel themselves forwards due to external rotating magnetic fields which act on the magnetic nanoparticles attached to the cells resulting in travelling waves. Protocols have been designed to create these multi-flagellated IRONSperm, to increase their velocity. During this study multi-flagellated IRONSperms were found and analysed on their velocity and the created thrust force for each individual flagella. The experiments showed the highest swimming speed for triple-flagellated cells of 13.81 Micron/s at 8 Hz, but that is just the tip of the iceberg. Looking at the propulsive forces for each of the flagella a velocity of 23.07 micron/s is expected at 1 Hz, but during the experiment only a velocity of 2.26 micron/s is measured. It seems that the interaction between the flagella plays an important role in the velocity of the cell. Better coordination and flagella being in-phase with each other shows a positive impact, which should be looked into further to optimize multi-flagellate propulsion in IRONSperm.





# Contents

<b>Abstract</b>	<b>iii</b>
<b>1 Introduction</b>	<b>1</b>
1.1 Motivation . . . . .	1
1.2 Goal of the thesis . . . . .	2
<b>2 Theory</b>	<b>3</b>
2.1 IRONSperms . . . . .	3
2.2 Traveling-wave propulsion . . . . .	4
2.3 Multiflagellate propulsion . . . . .	6
2.4 Time-reversal asymmetry . . . . .	8
<b>3 Method</b>	<b>11</b>
3.1 Set-up . . . . .	11
3.2 Measuring Method . . . . .	12
3.2.1 Velocity . . . . .	12
3.2.2 Propulsive force . . . . .	15
3.3 Analysing method . . . . .	15
<b>4 Results</b>	<b>17</b>
4.1 Velocity . . . . .	17
4.2 Wave-functions and propulsive force . . . . .	19
<b>5 Conclusions and Discussions</b>	<b>23</b>
5.1 Conclusions . . . . .	23
5.2 Discussion . . . . .	24
<b>References</b>	<b>27</b>
<b>Appendices</b>	

<b>A</b>	<b>Matlab Code</b>	<b>29</b>
A.1	Code for measuring Velocity . . . . .	29
A.2	Code for creating wave-functions and thrust force . . . . .	32

# Introduction

## 1.1 Motivation

Using microrobots to deliver drugs or chemical agents is a viable option to minimize the incisions in traditional surgeries [1]. The body itself uses many biological autonomous systems in the form of bacteria, algae and spermatozoa [2]. These deliverers are optimised by nature to be used in the human body and might provide a useful template [2]. IRONSperms cells are dead bovine sperm cells to which nanoparticles are electrostatically attached. Due to the particles the cells will obtain an additional characteristic which is a dipole moment. The dipole moment is used as an external stimuli which can be actuated by magnetic fields, making it possible to control the movement of the IRONSperm sample [3]. The IRONSperm cells move by rotating their body which will result in a propulsive force. The cells will move forward when the propulsive force will overcome the viscous force of the surrounding liquid. In circumstances with low Reynolds numbers this becomes particularly difficult [1]. When the Reynolds number is much lower than 1, in order of  $10^{-5}$ , viscous forces will be far greater than inertial forces. Time-reversal symmetry in the movement of the robots is necessary to overcome the difficulties in Reynolds numbers and need to use drag-based propulsive force [3]. The biological component of the microrobot gives room for flexibility and interaction with other cells in order to achieve time-reversal symmetry. The quality of the drug-delivery system is highly dependent of the ability to control the cell and the paired velocity [3]. To be able to reach all of the locations where drugs need to be delivered the control and velocity has to be sufficient also, because the cell is naturally biodegradable meaning the cell has a limited time to reach its destination. Therefore many studies tried to increase the velocity of IRONSperms by creating protocols to make IRONSperms with multiple tails [4]. Having multiple tails would increase the produced propulsive force while the drag force would remain similar. Creating a protocol for making IRONSperms which would reliably contain cells with multiple tails is a challenge but the experiments per-

formed during this thesis show remarkable results with cells that have multiple tails and respond to the magnetic field, see figure 1.1.

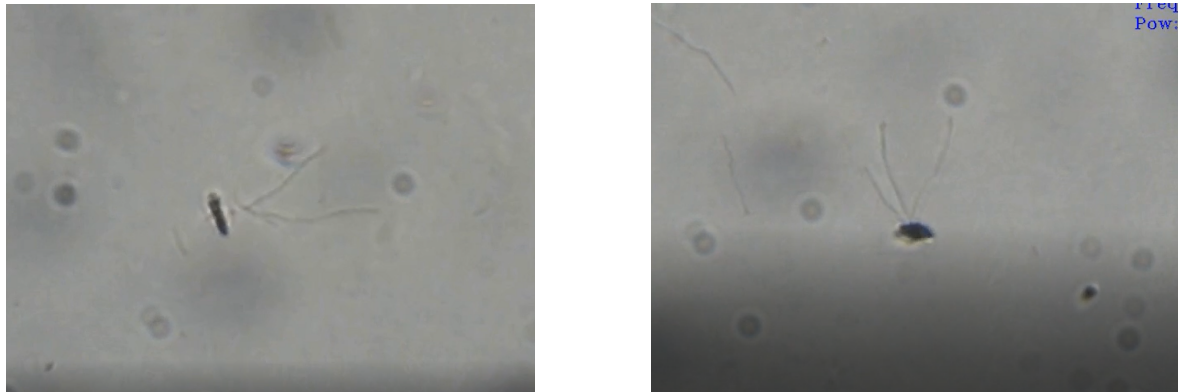


**Figure 1.1:** The left figure shows an IRONSperm with two flagella swimming to the left. The left figure shows an IRONSperm with three flagella swimming down.

## 1.2 Goal of the thesis

Cells with multiple tails come with an extra variable when analysing their movement. The tails provide propulsive thrust due to the lateral drag force they induce on their surroundings. The other tails however are also part of their surroundings, making the tails be obliged to interact with each other. The exact way the different tails interact is different for each cell since the way the tails are oriented is unique for every IRONSperm cell. The impact of these interactions on the velocity is interesting for using multi-flagellate cells in the future. Multi-flagellate sperm cells are bundled by using apical hooks position at the heads [5]. Sperm cells with multiple tails are made out of different cells with unique tails making each multiflagellate unique. With enough samples the efficiency of the tails can be analysed and the consequences on the cell's velocity can be estimated. First, the overall velocity of the cell will be measured using the recorded videos of the actuated cell under the microscope. secondly, the individual tails of the multiflagellate cell are characterized to calculate their independent propulsive thrust. With these results, the research questions which are sought to be answered in this thesis are:

What is an IRONSperm?

How does an IRONSperm swim?

What is the result of having multiple tails on an IRONSperm?

How do separate flagella on a single cell interact with each other?

How is multi-flagellated propulsion different then single-flagellated propulsion?

# **Theory**

## **2.1 IRONSperms**

A rotating magnetic field with a constant frequency is used to actuate the IRON-Sperm cells. The nanoparticles, made of iron oxide, which are attached to the cell respond to the magnetic field and will try to follow its rotation [4]. The cell will then in turn also follow this rotation. The position and distribution of the nanoparticles is different for each cell, as shown in figure 2.1. The middle cell in figure 2.1 only has particles attached to the head where the right cell also has more iron oxide particles attached to the body, causing the cells to have different responses to the magnetic field [4].

The motion characteristics of a magnetically actuated passive filament is different from that of a live cell. A live sperm cell uses active contractile elements to induce a bending moment in the filament [6]. A passive flagellum induces a propagating wave initiated from boundaries [7]. In addition, a filament of an IRONSperm has significantly different properties because the nanoparticles modify the bending stiffness and weight of the filament [1]. To understand what these exact motion characteristics entail a cell with a single tail is explained using the equations below. A cell with multiple tails will be obtained from merging cells with single tails together, thus these motion characteristics will transfer over to a multiflagellate cell. The governing equations of the deformation of the filament can be obtained starting with the general balance of forces and the limits of deformation. The deformation is governed by the balance of magneto-elastic and drag forces, ultimately resulting in a traveling wave [6].

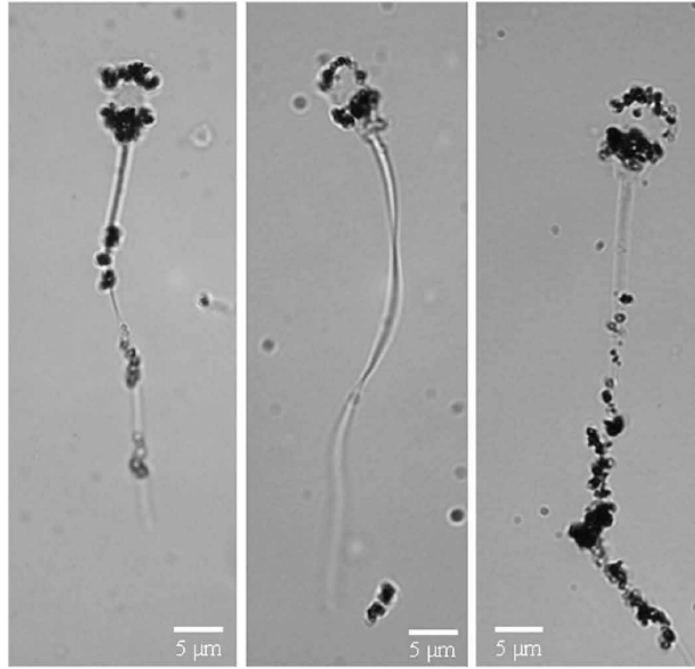


**Figure 2.1:** Microscopic images of three different IRONSperms. The black dots show the iron oxide particles attached on the head and body of the cells [4].

## 2.2 Traveling-wave propulsion

An IRONSperm cell makes use of traveling-wave propulsion to swim. An undulatory system can propel itself if the body pushes harder than the drag force on the body [6]. If a tail with length  $l$  and bending stiffness  $\kappa$  is deforming such that it produces a transverse bending wave initiated at its proximal end, the steady-state solution of the balances of forces along the uniform filament will only depend on the sperm number [7]:

$$Sp = l \left( \frac{\xi_{\perp} \omega}{\kappa} \right)^{1/4}, \quad (2.1)$$

where  $l$  is the length of the tail,  $\xi_{\perp}$  is the normal drag coefficient,  $\omega$  is the angular frequency and  $\kappa$  is the bending stiffness. The optimal sperm number is equal to approximately 2.1 for a sperm cell with 1 tail [7]. For a cell with multiple tails this sperm number will be different, but because a cell with multiple tails will be constructed from cells with single tails this value will still be accounted for. Before we look at cells with multiple tails we first assess the equation of deformation of single tail. We consider a sphere-shaped head and consider the head to be the only magnetic part of the cell. The nanoparticles attach in greater numbers to the head than to the rest of the body with as a result that in practice the head has the highest magnetization [7]. The head is attached to a flexible filaments with length  $l$  and bending stiffness  $\kappa$ . The cell is externally actuated by a magnetic field  $B(t)$  and angular frequency  $\omega$ . The

equations of deformation are:

$$\kappa \frac{\delta^4 y(x, t)}{\delta x^4}(x, t) = \xi_{\perp} \frac{\delta y}{\delta t}(x, t), \quad (2.2)$$

$$y(0, t) = 0, \frac{\delta y(0, t)}{\delta t} = y_0 e^{i\omega t}, \frac{\delta^2 y(L, t)}{\delta t^2} = 0, \frac{\delta^3 y(L, t)}{\delta t^3} = 0, \quad (2.3)$$

$y(x, t)$  is the position and therefore deformation of the filament relative to a fixed frame of reference. The boundary equations mean that the head will remain stationary relative to the fixed frame and the rest of the tail will follow a constant circular motion. The energy needed to rotate the filament is fed by the angular displacement of the magnetic head due to the rotating magnetic field [7]. Equation 2.8 shows in the first term the magneto-elastic force and in the second term the drag forces. Using the boundary conditions shown in equation 2.3 it returns the following steady-state solutions:

$$\frac{\delta y}{\delta t} = i2\pi f e^{i2\pi f t} \left( \sum_{j=1}^4 A_j e^{r_j x} / j_0 \right), \quad (2.4)$$

$$\frac{\delta y}{\delta x} = \frac{1}{l_0} e^{i2\pi f t} \left( \sum_{j=1}^4 A_j r_j e^{r_j x} / j_0 \right). \quad (2.5)$$

From the steady-state solutions in equations 2.4 and 2.5 it shows that the time-derivative is linearly dependent of the angular frequency [7]. So, when the frequency will be twice as large the lateral velocity will also be twice as large. With known length  $L$  for the filament the propulsive thrust can be calculated as follows:

$$f = (\xi_{\perp} - \xi_{\parallel}) \lim_0^L \frac{\delta y}{\delta t} \frac{\delta y}{\delta x} dl = i2\pi f (\xi_{\perp} - \xi_{\parallel}) e^{i4\pi f t} \sum_{j=1}^4 \sum_{k=1}^4 \frac{A_j A_k r_k}{r_j + r_k} e^{(r_j + r_k)x Sp/L}. \quad (2.6)$$

This equation explains the basic principle behind drag-based thrust that the filament will propel forward only when the lateral force pushed against the surrounding fluid is higher than the drag force parallel to the filament. The ratio between these resistive coefficients is  $\frac{\xi_{\perp}}{\xi_{\parallel}} \approx 2$  [7]. Meaning that in equation 2.6  $(\xi_{\perp} - \xi_{\parallel})$  will almost always be positive resulting in a positive propulsive thrust. The propulsive for different cells is dependent on the sperm number  $Sp$ , which is dependent of 4 variables; the length of the flagella, the normal drag coefficient, the angular frequency of the cell and the bending stiffness.

In figure 2.2 the wave pattern and the corresponding propulsive thrust is plotted for three different values. For a sperm number lower or equal to 1 the propulsive force is different only along the length flagellum [7]. This shows that the flagellum is not producing a wave, meaning the flagellum is rigid and doesn't produce a net force. When  $Sp$  is increased the location of the maximal thrust on the flagellum changes

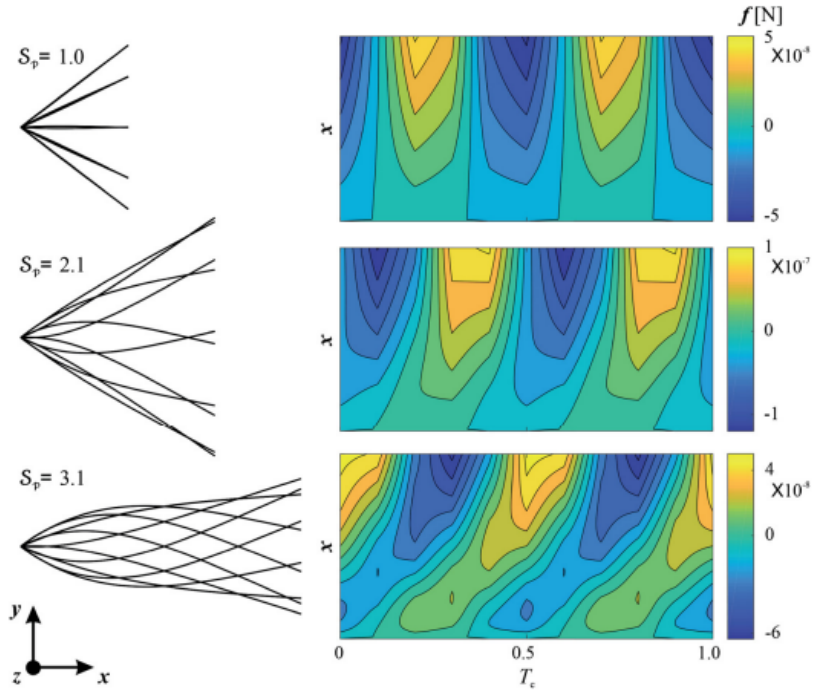


**Figure 2.2:** Flagellar wave-patterns and the corresponding propulsive thrust for three different sperm numbers; 1.0, 2.1 and 3.1. A sperm number of 2.1 shows to be the optimal value providing the most thrust [7].

with time as seen in figure 2.2. The higher the sperm number gets the more curved the progression of the shift becomes. These wave patterns are calculated over on complete beat cycle from which the total average propulsive force can be calculated over one cycle using:

$$\langle f \rangle = \frac{1}{T_c} \int_0^{T_c} f dt. \quad (2.7)$$

Figure 2.2 shows in the flagellar wave-pattern of the flagellum with a  $S_p$  of 2.1 that the areas of positive propulsive thrust is larger than the areas of negative propulsive thrust. Using equation 2.7 it can be shown that an overall positive forward propulsion is obtained. For the optimal sperm number a balance has to be achieved where the flagellum curves enough to obtain a net propulsion but too much to a point where it loses too much energy curving the flagellum [7]. The optimum value is for the sperm number at 2.1 producing the highest propulsive thrust [1], [7].

## 2.3 Multiflagellate propulsion

For micro-organisms which reside in an environment with Reynolds number of order  $10^{-5}$  reciprocal motion is incapable of generating forward thrust [8]. For this reason, these organisms had to evolve to optimize their propulsive structures in order



to gain forward motion and overcome the limitations of the low Reynolds number [8]. Multiflagellar configurations showed to be a profitable solution. Studies have examined multiflagellate systems like *Chlamydomonas*, a biflagellate algae, and the *Giardia lamblia*, an impressive octo-flagellated eukaryote [8]. Unlike the symmetric multi-flagellate arrangements there are even more complex systems like the quadri-flagellated *T. foetus*. The *T. foetus* has four flagella, from which three are position forward in front of the cell. The fourth flagellum is curving back along the body, see figure 2.3, attaching at several points on the body and providing a propulsive thrust at the back of the cell [8]. The exact theory behind multi-flagellated structures is still studied intensively, but as has been showed in figure 2.3 the propulsive system gets complex and is unique for every micro-organism. This causes for an unique interaction between flagella. The study about the *T. foetus* showed that the three anterior flagella were responsible for 87% of the forward thrust [8]. But for this to the case the timing or phase of beating was shown to have significant effect on the provided propulsion. Having multiple flagella shows to be advantageous for creating more velocity, but only when the collaboration between the flagella is highly coordinated [8].

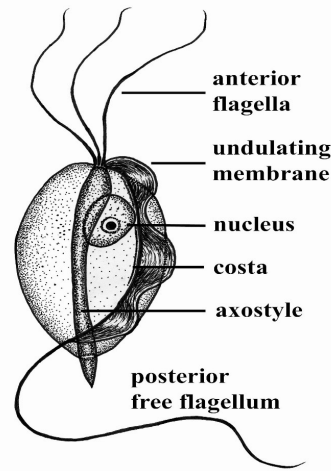


**Figure 2.3:** Morphologic structure of a *T. foetus* (*Titrichomonas foetus*) showing the four flagella and their orientation [8].

A force balance can be constructed between the heads and flagellum to predict the swimming velocity from the propulsive forces of multiple flagella. This force balance for multi-flagellate cells looks as follows:

$$F_h + F_{f1} + F_{f2} + \dots = 0, \quad (2.8)$$

where  $F_h$  represents the drag force of the head which gives a negative force. This forward drag force is calculated as follows:

$$F_h = \eta CV_x, \quad (2.9)$$

where  $\eta$  is the medium viscosity,  $C$  is the geometric coefficient of the head and  $V_x$  is the forward velocity of the entire cell.  $F_f$  is the thrust force provided by all the flagella combined, represented for one flagella by equation 3.1.

## 2.4 Time-reversal asymmetry

Passive flagella can swim in an environment with a low Reynolds number because of their chiral geometry [6]. A chiral shape is a shape that cannot be superimposed into and is not identical to the mirror image of the shape. This chirality is necessary for the flagella because of its property to not be time-reversal symmetrical. The total propulsive force can be related to the perpendicular and parallel force by this equation [6]:

$$\delta f = \delta f_{\parallel} \sin \theta - \delta f_{\perp} \cos \theta = (\xi_{\perp} - \xi_{\parallel})U \sin \theta \cos \theta \delta l. \quad (2.10)$$

In order to determine if the cell actually propels forward  $\delta f$  is integrated over an entire periodic cycle. If we consider an example where the velocity is  $U$  with configuration  $\theta$  and compare this with a cell with velocity  $-U$  with the same configuration we obtain the following:

$$\begin{aligned} U, \theta &\Rightarrow \delta f = (\xi_{\perp} - \xi_{\parallel})U \sin \theta \cos \theta \delta l, \\ -U, \theta &\Rightarrow \delta f = -(\xi_{\perp} - \xi_{\parallel})U \sin \theta \cos \theta \delta l. \end{aligned} \quad (2.11)$$

In this example the average  $\delta f$  is 0, meaning that going from a forward velocity of  $U$  to a similar velocity backwards requires 0 net force. In a periodic cycle  $U$  and  $-U$  will cancel each other out and result in a motionless cell. To overcome this time-reversal symmetry the configurations for a velocity forwards and backwards should be different such that the average propulsive force is not equal to 0 [6]. Therefore, an example where the configuration for velocity is  $U$  with configuration  $\theta$  and for velocity  $-U$  and configuration  $\pi - \theta$  should look as follows:

$$\begin{aligned} U, \theta &\Rightarrow \delta f = (\xi_{\perp} - \xi_{\parallel})U \sin \theta \cos \theta \delta l, \\ -U, \pi - \theta &\Rightarrow \delta f = -(\xi_{\perp} - \xi_{\parallel})U \sin \pi - \theta \cos \pi - \theta \delta l, \\ &= (\xi_{\perp} - \xi_{\parallel})U \sin \theta \cos \theta \delta l. \end{aligned} \quad (2.12)$$

From this example with a different configuration when the motion is in the opposite direction the propulsive force is equal. Resulting for the entire time-periodic cycle of the flagella that the average propulsive force is not equal to 0 and there is movement. As said before, to have a cell with a geometry where the configuration is different in which direction the motion is the filament of the cell needs to have a chiral shape. This is to not be time-reversal symmetric and be able to produce a netto propulsive thrust.



# Method

## 3.1 Set-up

A microscope system with an attached camera is used to analyze the IRONSperms. On this microscope system there are Helmholtz coils placed, see figure 3.1, which are used to induce a magnetic field. The samples of IRONSperms are placed on a microscope slide or as a hanging droplet under the microscope in between the magnetic coils. The following parameters of the magnetic field can be changed: field strength, direction of the field, rotating frequency of the field and the angle of the rotating field between the direction of the field. The IRONSperm samples are preserved in cooling temperatures and the cells are contained in a water-like substance. The sample can be placed under the microscope in two different ways; a droplet on a slide and a hanging droplet. When a droplet of the sample is placed on the microscope slide using a pipet the droplet will start to slowly spread over the slide. Because the cells are heavier than the fluid they will sink to the bottom. This makes it harder to keep them into focus and they can get stuck to the slide causing the cells to not be able to move anymore. The hanging droplet is a method where the droplet is being kept intact. Because the droplet is much thicker and doesn't spread out that much compared to a droplet on a slide the cells are more likely to cluster making it difficult to get them to move on their own. For this experiment the droplet on a slide is used, because the droplet will spread out over the slide it becomes easier to analyze a single cell and measure its velocity.

The vial, shown in figure 3.1, used in the experiments contain IRONSperm coated with  $1\text{-}\mu\text{m}$  iron oxide particles. The cells in the vial are created using a method to specifically increase the amount of bundled cells. Sperm cells have apical hooks, see figure 3.2, located on their heads. When sperm cells come in contact with each other they can attach themselves to each other forming a bundle of cells. Experiments show that this phenomenon occurs at a higher rate when the cells are in a high-viscosity fluid. To create IRONSperm with a higher chance of containing bun-



**Figure 3.1:** The first picture shows the set-up showing the microscope on which the helmholtz coils are attached. The samples are placed between the coils to be examined. The second picture shows vial containing the used sample. The samples are contained in cooling conditions.

dles this property is used. Live bovine sperm cells are put in an environment with a high viscosity to stimulate the cells to form bundles. Afterwards the cells are coated with the rice particles and can be analysed as IRONSperm, which results in a cell seen in figure 3.3.

## 3.2 Measuring Method

### 3.2.1 Velocity

From the measurements we want to obtain two variables; the velocity of the cell and the wave-functions of the tails to be able to calculate the propulsive force. To analyse the velocity of the cell a step-response is done. During the step-reponse the frequency of the field is varied. The step-reponse will start at 1 Hz and is increased until the cell is no longer responding to the direction of the magnetic field. The cell will no longer be considered responding when the cell can not follow the velocity of the rotating magnetic field and will start to catch behind, to eventually be visually oscillating rather than rotating. To measure the velocity at certain frequencies the cell is recorded for around 8-10 seconds per frequency. During the recording the microscope is not moved which makes it possible to determine the beginning- and endpoint of the cell in the frame. The time between the beginning- and endpoint is known, therefore the velocity can be calculated. A Matlab-script is used to determine

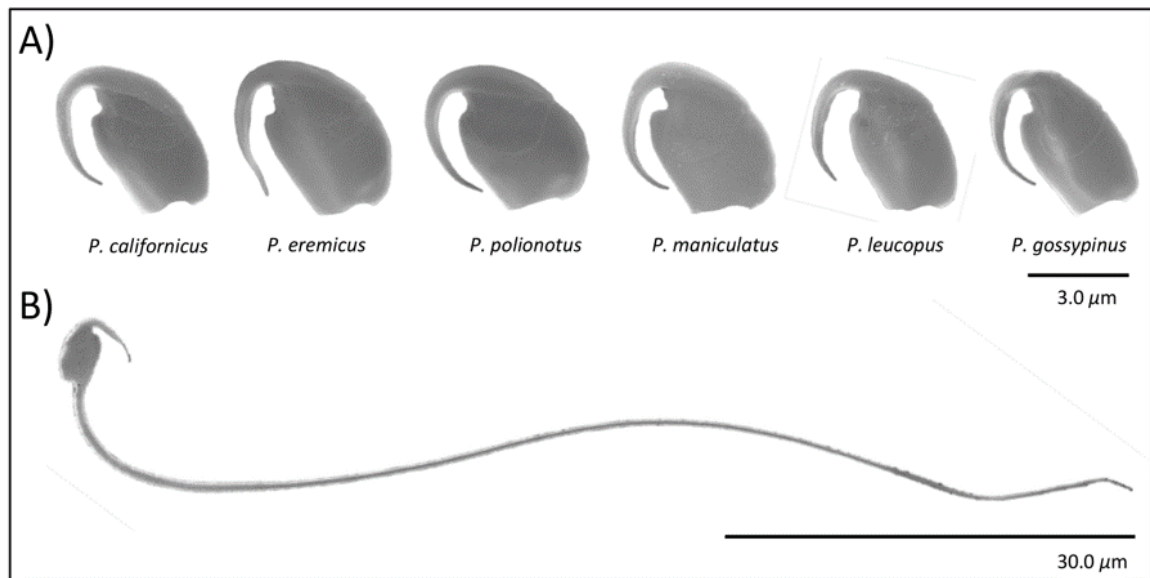


**Figure 3.2:** Representative image showing different apical hooks and a full sperm cell showing the proportions [5].

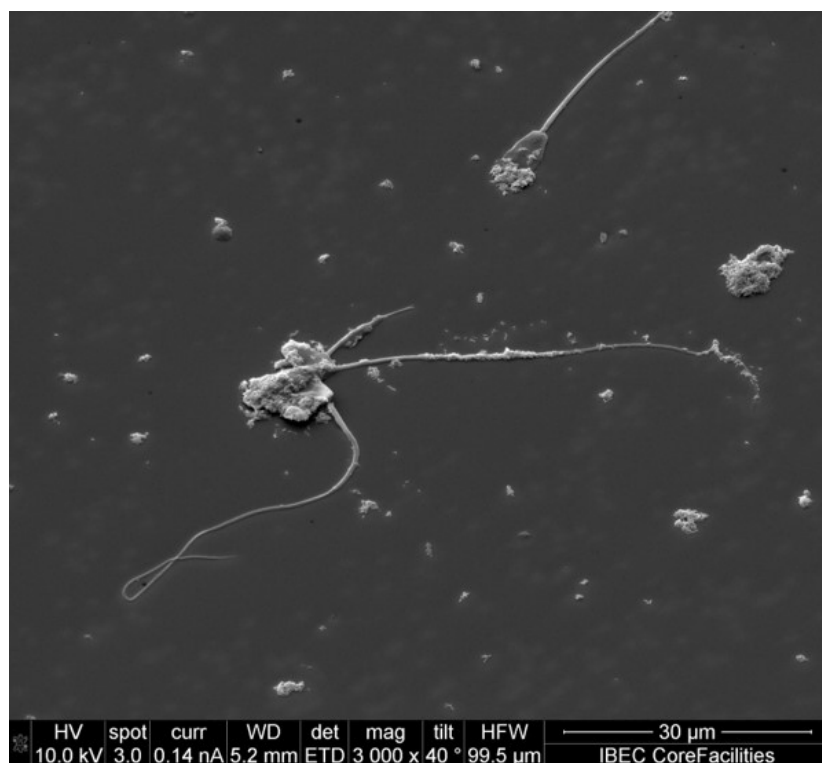


**Figure 3.3:** Microscopic cyro-image of a multi-flagellated cell from the sample used in the experiments. Three cells are attached to each other at the head using their apical hooks forming a cell with three flagella.

these points and calculate the velocity, which is shown in the appendix. The beginning and end points would be chosen by clicking manually on the head of the cell, this is performed in duplo to minimize inaccuracies. The strength of the magnetic field is set at 4 mT and the angle of the rotating field is  $90^\circ$ . On the interface seen in figure 3.4 there is a blue and red line which indicate the orientation of the magnetic field. The blue line is the rotation axis of the field and the red line is the direction of the magnetic field which is rotating around the blue line. The direction of the rotation axis would be set to be either one of the cardinal directions. This would simplify the way the velocity of the cell could be measured. To be able to quantify the velocity of the cells from the recordings, the ratio between the pixels and the real size must be determined. This is done using a ruler, placed under the microscope. The actual lengths between points on the ruler is known. The actual size of one pixel can then be obtained from an image of the ruler, when the same equipment and settings are used.

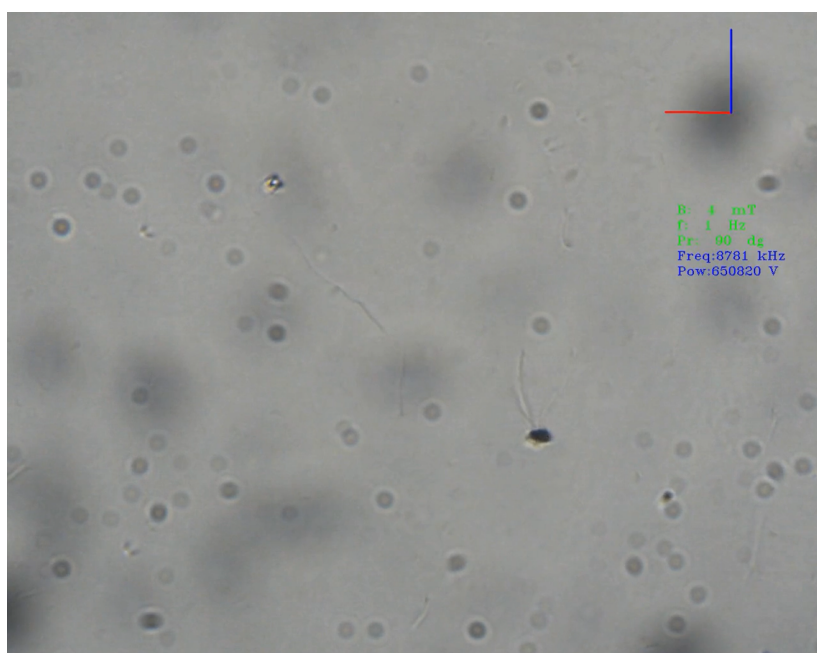


**Figure 3.4:** Raw screenshot of the recordings showing the interface. On the top-right there is a blue line showing the rotating axis of the magnetic field and the red line pointing parallel to the actual direction of the magnetic field. The interface also shows the field strength, rotating frequency and rotating angle in green. The blue text contains information about the helmholtz coils. The black dots in the screen are the result of noise, distortion or filth on the lenses.



### 3.2.2 Propulsive force

To measure the wave-functions of the tails only a recording is needed with the magnetic field at a single frequency. However, to be able to analyse the wave-function the flagellum/flagella of the cells need to be tracked. To track a flagellum of the cell, the flagellum will be traced manually on 40 points, using the code in the appendix. For the flagellum to be tracable a high resolution of the flagellum is needed. Therefore, the frequency is set at 1 Hz to minimize motion blurring and vibrations of the fluid. The cell sinks during the recordings due to gravity, so the cell is kept in focus manually.

## 3.3 Analysing method

After the flagella in the frames are traced, see figure 3.5, the wave-functions are constructed from the aforementioned 40 points.



**Figure 3.5:** Image showing a cell with two tails of which one is traced using 40 data points. From these data points the wave-function and eventually the propulsive force can be calculated.

From the wave-functions the following equation for the forward thrust can be used:

$$F = \int_0^\lambda \left( (\xi_\perp - \xi_\parallel) \frac{\delta y}{\delta t} \frac{\delta y}{\delta x} \right) dx. \quad (3.1)$$

The drag coefficients for the forward thrust is calculated as follows:

$$\xi_{\perp} = 4\pi\mu/\left(\ln\left(\frac{l}{r}\right) + 0.193\right), \quad (3.2)$$

$$\xi_{\parallel} = \xi_{\perp}/2, \quad (3.3)$$

for  $\mu$  the viscosity of water is used. In equation 3.2  $l$  is the length of the flagella and  $r$  the radius, these are chosen respectively at 70 microns and 5 microns.

From these results can be determined what the relation is between the overall velocity of the cell and the propulsive forces of the separate tails. More tails will result in a higher overall forward force but, as explained before, a cell with multiple tails will also provide mutual interaction.

# Results

## 4.1 Velocity

For the velocity 9 cells are used; 3 cells with 1 tail, 3 cells with 2 tails and 3 cells with 3 tails. Examples of each can be seen in the figure below.



**Figure 4.1:** Three microscopic images of three different cells containing one, two and three flagella.

For each of the cells a step-response is obtained. Before the velocity can be measured the actual size of the images has to be determined. A ruler is placed under the microscope as shown in figure 4.2.

The ruler showed that 2.2 pixels are equal to 1 micron. The step-responses of the cells are plotted in Matlab as such:

The average velocities of cells with the same amount of tails is then plotted together in figure 4.7. The same is done for the standard deviation. The cells with 1 and 2 tails show a step-out frequency at around 3-4 Hz. The cells with 3 tails show a higher set-out frequency at 7-8 Hz. Also the velocities of the cells with 1 and 2 tails are very similar where the cells with 1 tail show an even higher average velocity. The maximum average velocity of the cells with 1 tail is 13.04 Micron/s and that of the cells with 2 tails is 10.68 Micron/s. The velocity of the cells with 3 tails has a maximum of 13.81 Micron/s.

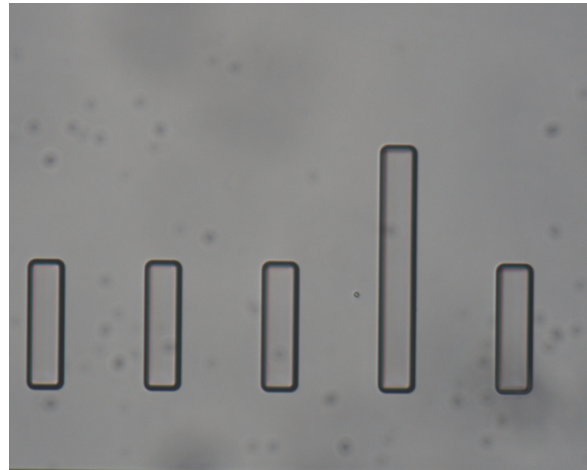


**Figure 4.2:** Microscopic image of the ruler placed under the microscope in order to measure a scale for the images. The real distance between two small lines is 100 micron.

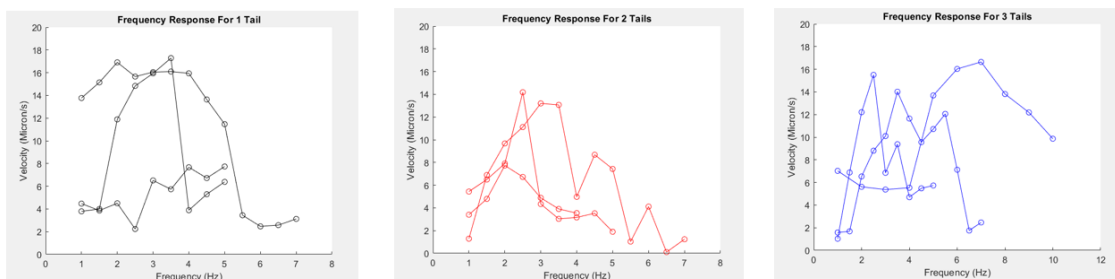


**Figure 4.3:** Three graphs of the step-responses for each amount of flagella each consisting of three lines. The first graph shows the step-responses for the cells with 1 flagellum, the second of these with 2 tails and the third of these with 3 tails.

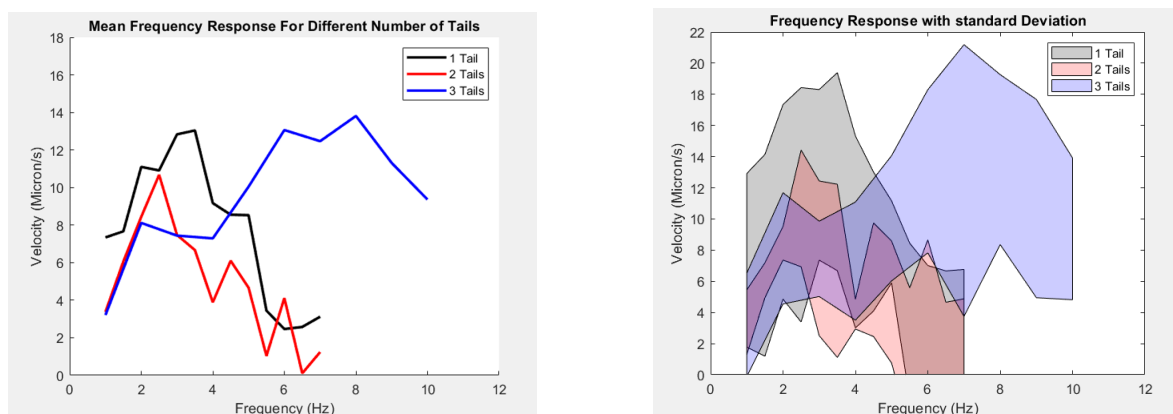


**Figure 4.4:** The first graph shows the average velocities during the frequency response for each amount of tails. The second graph also shows the corresponding standard deviation.

Tails	Maximum velocity (Micron/s)	Frequency (Hz)
1	13.04	3.5
2	10.68	2.5
3	13.81	8

## 4.2 Wave-functions and propulsive force

From the tracked flagella the wave-functions for each of the flagella of 3 cells are constructed. 3 cells with 1, 2 and 3 flagella are analysed. The recordings used for tracking the flagella are cropped to enlarge the cell and ease the tracking process.

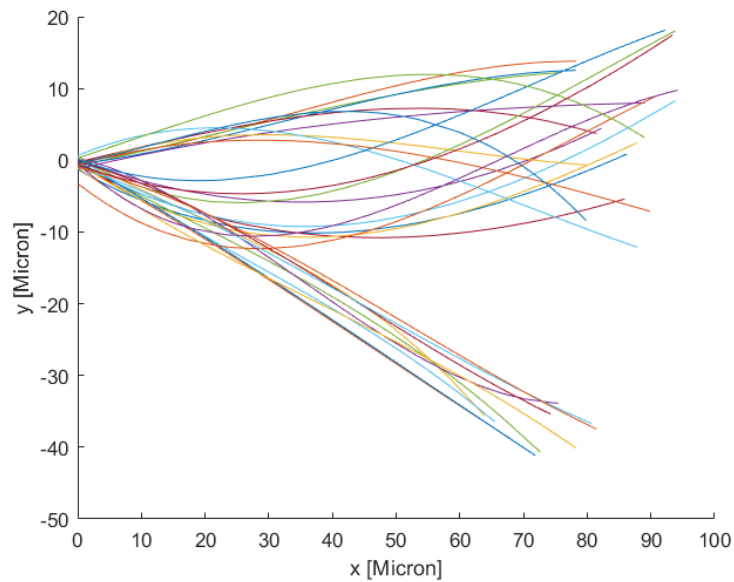


**Figure 4.5:** Fitted wave-functions for the cell with a single flagellum. The flagellum shows to have an average length of 87 micron.

Using equation 3.1 the propulsive force for each of the flagella is calculated.

Using these calculated thrust forces we can calculate the forward velocity from these using the force balance in equation 2.8. We consider an ellipsoid head.

Tails	Calculated Velocity (Micron/s)	Real Velocity (Micron/s)
1	8.33	30.29
2	26.91	7.48
3	23.07	2.26

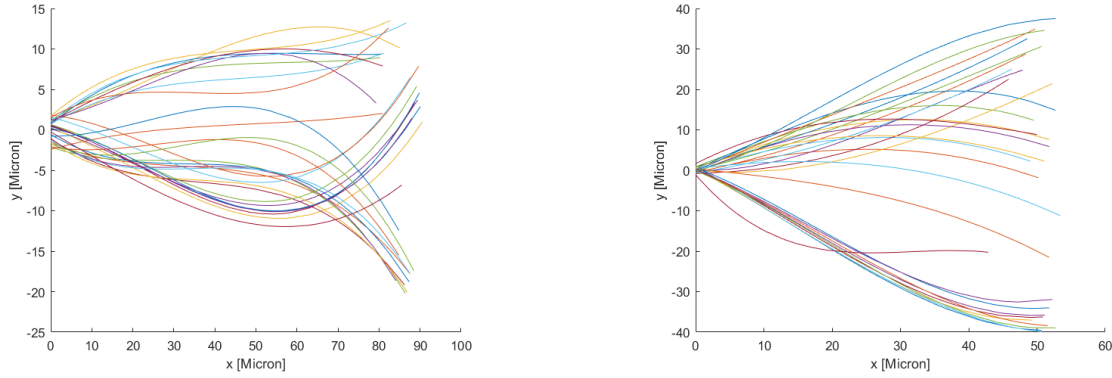


**Figure 4.6:** Fitted wave-functions for the cell with two flagella, each graph corresponding with one of the flagella. The first flagellum has an average length of 89 microns and an amplitude of around 15 microns. The second flagellum has a lower average length of 59 microns but does have a higher amplitude.

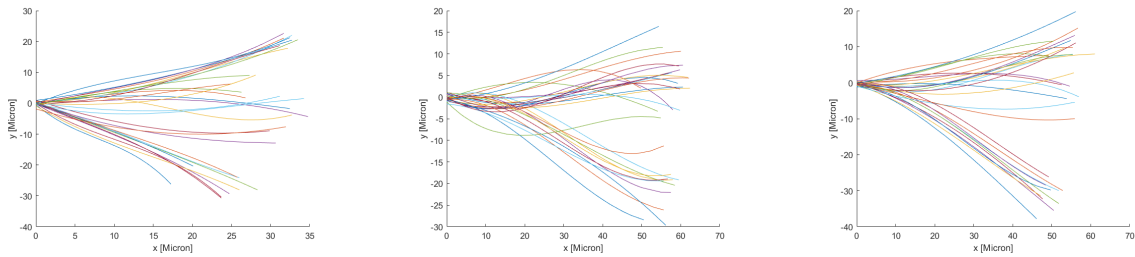


**Figure 4.7:** Fitted wave-functions for a cell with three flagella, each graph corresponding with one of the flagella. The first flagellum has a lower average length then the other two flagella of 35 microns. The second and third flagella have an average length of 60 and 57 microns. The amplitude of the first flagella is around 25 microns. The amplitude of the second and third flagella is lower then that of the first flagella with an amplitude of around 20 microns.

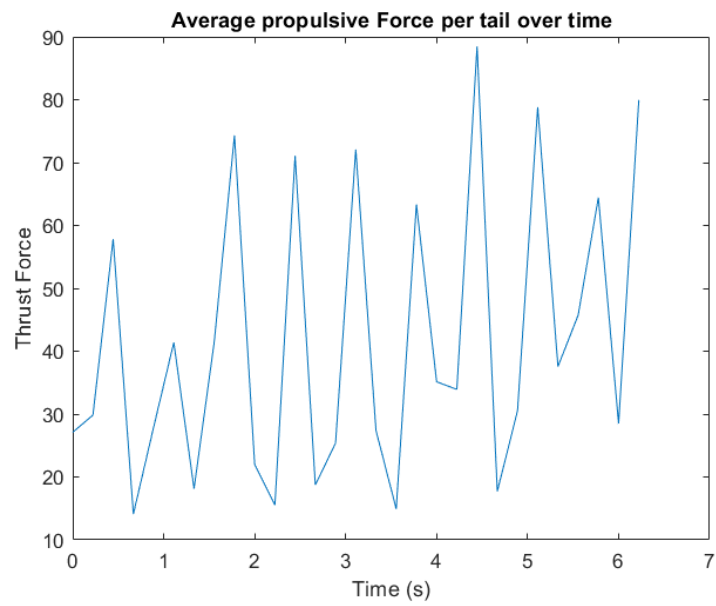


**Figure 4.8:** Thrust force calculated from the fitted wave-functions plotted over time for a cell with a single flagellum.

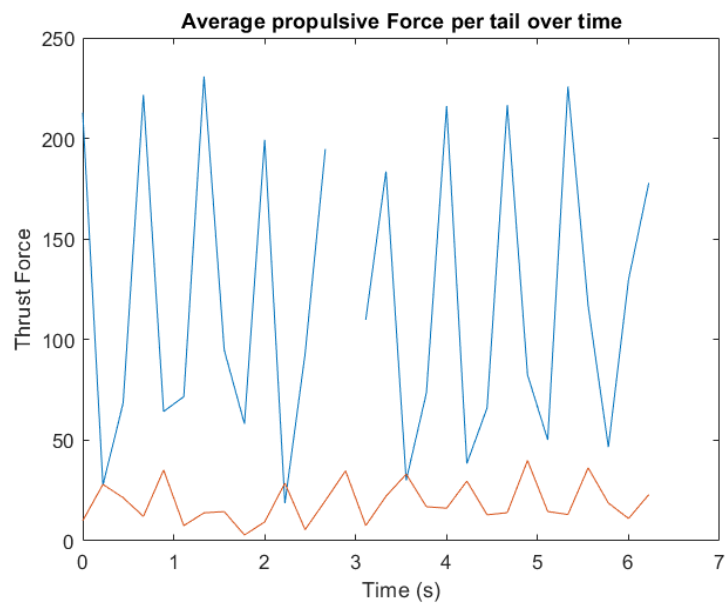


**Figure 4.9:** Thrust force calculated for two flagella from the fitted wave-functions plotted over time.

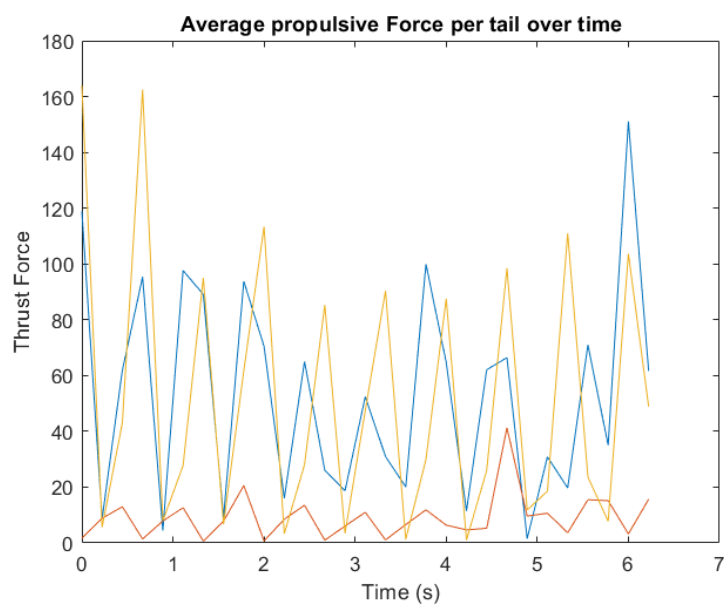


**Figure 4.10:** Thrust force calculated for three flagella from the fitted wave-functions plotted over time.



# Conclusions and Discussions

## 5.1 Conclusions

The velocity of the multi-flagellated show promising results. Especially the triple-flagellated cells had the highest average velocity of 13.81 Micron/s. The double-flagellated cells however only achieved a highest average velocity of 10.68 Micron/s, significantly lower than even the single-flagellated which had a highest velocity of 13.04 Micron/s. The difference between the highest average velocity of the single- and triple-flagellated cell is only 0.77 micron/s but an important difference is the frequency at which this was achieved. The highest velocity of the single-flagellated cells was at 3.5 Hz while the triple-flagellated cells had their highest velocity at 8 Hz. This discrepancy tells that the triple-flagellated cells appears more stable and can easier cope with a higher amount of energy input from a higher frequency. From the graph showing the standard deviation of the velocity of the different sets of tails we can conclude that the sample size is not large enough yet to make a clear distinction between the velocity of the cells.

We also measured the propulsive force for each of the flagella of 3 cells using their wave-functions. The most noticable result of the graphs of the propulsive force is their periodic nature. All of the graphs show short peaks of around 2 times their average propulsive force and promptly after a short valley. In figure 4.9 the force of both tails are out of sync, while in figure 4.10 all of the three tails seem to be fairly in-sync. The flagella for the triple-flagellated are coordinated better which can be an explanation for the higher velocity. The force of the single-flagellated cell is not even half of the most propulsive flagella of the multi-flagellated cells. Still, the velocity of the single-flagellated cell is only 6% lower than that of the cell with three flagella. Multi-flagellate cells show higher velocities provided that the flagella work coordinated, but also lose a lot of the propulsive force.

The table showing the calculated and real-life propulsive is interesting because it shows opposite trends. The calculated velocity, from the thrust force of each tail, is increasing. When looking at the force balance this makes total sense, since the force provided by the flagella is increasing but the drag force of the body is kept the same. When  $F_f$  increases,  $V_x$  increase as well. However, when looking at the real velocity it decreases when the amount of flagella increases. There seems to be a missing variable in the force balance which increases when the amount of flagella increases. It seems that the interaction between the flagella plays a role in the velocity of the cell which should be looked into further to optimize multi-flagellate propulsion in IRONsperm.

## 5.2 Discussion

For constructing the step-responses only 3 samples are used for each amount of tails. This can give an indication of the velocity, but when looking at the standard deviation of the step-reponses there is a wide-range of uncertainty. The problem however during the experiment is that there was a limited amount of sample. only a single vial showed to contain cells with multiple flagella and was suitable to perform experiments on. For increasing the liability of the results more vials using the same protocol should be made to increase the sample size.

Because only one vial contained usable cells, only the single vial was used, but using different vials with multi-flagellate cells should have a positive effect on the experiments. Using different vials could both show the liability of the protocol for creating cells and the variance there is between multi-flagellate cells.

For the step-responses that were made during this thesis there is a difference between the length of the step-responses of the different cells. The step-responses were made to be able to analyse the swimming-velocity of the cells. Therefore, the cells were measured for the time that they were actually responding to the magnetic field and using the propulsion of the tails by rotating them to propel forwards. When these swimming characteristics were not present anymore the step-responses were stopped. But, especially at high frequencies, judging these characteristics becomes challenging. For example, during one of the step-responses the cell started to have a lot of uncoordinated movement to an extent that the cell was moving more to the sides than it was moving forward. But the forward velocity was still higher than the velocity it had at some lower frequencies.

For creating the wave-functions the flagella are tracked using Matlab. On different frames of the cell the flagella is tracked at 40 points. The precision in tracking of

the flagella is challenging due to the difference in quality of the video-frames. The frames capture the cells which move in 3 dimensions. Because the flagella are rotating they will move in and out of the frame causing the flagella to get in and out of focus. This causes for the flagella to be partly or entirely out of focus, making it hard to correctly track the entire flagella. Getting higher resolution recordings can greatly increase the tracking quality and with it the credibility of the calculated thrust forces. This could also have made it possible to analyse the produced thrust at higher frequencies. Especially since eventually there is a shift where the velocity of the multi-flagellate cells gets higher than that of the single-flagellated cells. Analysis at these higher frequencies can give an insight in what makes the multi-flagellated cells more efficient at these frequencies.

As shown in the theory a multi-flagellated cell accounts for a lot more different factors which influences its velocity. For this thesis we looked at the individual propulsive force for each of the tails. But the tails will interact with each other causing them to, for example, bump into each other or create a strong local fluid vortex. For further studies it could be promising to look at the synchronising effect of flagella and the influence on the cell's velocity.

For the experiments cells were chosen from the samples which had a typical appearance. The cells that were chosen all had a single large head, had their flagella pointing in the same direction and moved forward using the magnetically induced rotation from the flagella. Those cells were chosen because they have the highest chance on actually showing results and have a response to the step-response. But, there are different ways the flagella can work to produce a propulsive thrust. Cells like in figure 5.1 and 5.2 are definitely present in the samples and might show remarkable swimming techniques when analysed further.

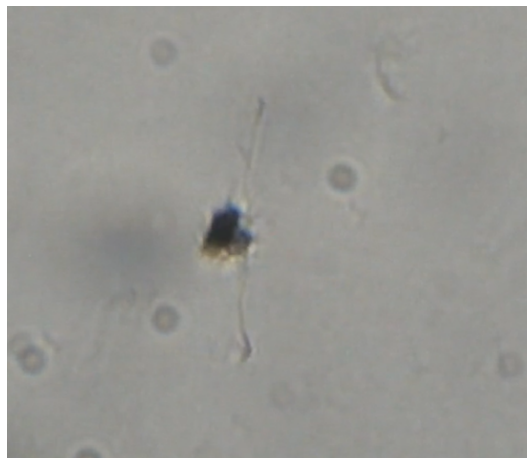
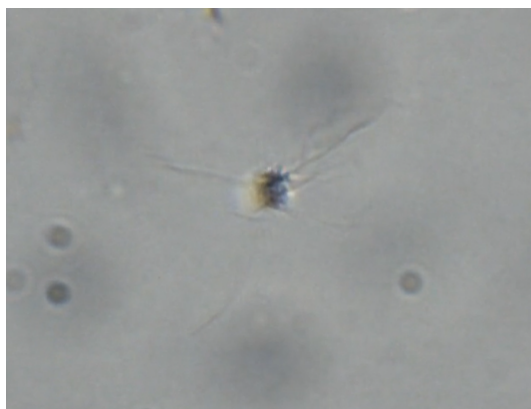


**Figure 5.1:** Both images show atypical cells found during the experiments. The first image shows a cell with around 8 flagella all pointing to a different direction. The second image shows a cell with 2 flagella being positioned almost exactly opposite of each other.

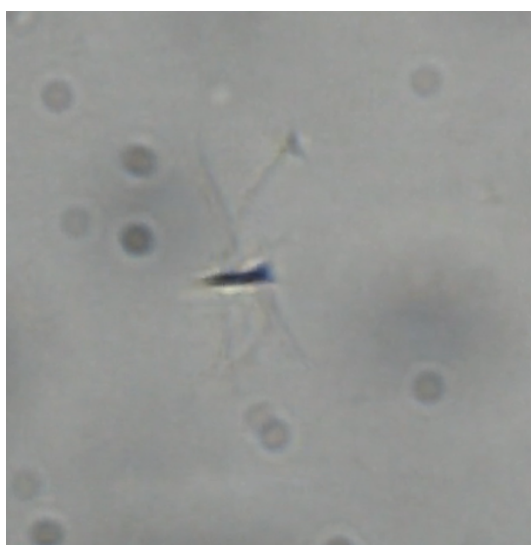


**Figure 5.2:** Both images show atypical cells found during the experiments. The first image shows a cell with around 6 flagella from which 2 point upwards while the other flagella point in the opposite direction. The second image shows a cell with 7 flagella pointing in the same direction.

# Bibliography

- [1] J. M. S. Dias, D. Estima, H. Punte, A. Klingner, V. M. Lino Marques, and I. S. M. Khalil, "Modeling and characterization of the passive bending stiffness of nanoparticle-coated sperm cells using magnetic excitation," *Advanced theory and simulations*, [www.advtheorysimul.com](http://www.advtheorysimul.com), 2022.
- [2] V. Magdanz, J. Vivaldi, S. Mohanty, A. Klingner, M. Vendittelli, J. Simmchen, S. Misra, and I. S. M. Khalil, "Impact of segmented magnetization on the flagellar propulsion of sperm-templated microrobots," 2021.
- [3] V. Magdanz, J. Gebauer, D. Mahdy, J. Simmchen, and I. S. Khalil, "Sperm-templated magnetic microrobots," *Proceedings of MARSS'19*, 2019.
- [4] V. Magdanz, I. S. M. Khalil, J. Simmchen, G. P. Furtado, S. Mohanty, J. Gebauer, H. Xu, A. Klingner, A. Aziz, M. Medina-Sánchez, O. G. Schmidt, and S. Misra, Eds., *IRONsperm: Sperm-templated soft magnetic microrobots*, 2020.
- [5] K. A., Wilke, L. M., Fisher, and H. S., "Apical sperm hook morphology is linked to sperm swimming performance and sperm aggregation in peromyscus mice," *Cells*, vol. 10, no. 9, 2021. [Online]. Available: <https://www.mdpi.com/2073-4409/10/9/2279>
- [6] I. S. Khalil, A. Klingner, and S. Misra, *Chapter 1 - Introduction: Soft microrobots*, I. S. Khalil, A. Klingner, and S. Misra, Eds. Academic Press, 2021. [Online]. Available: <https://www.sciencedirect.com/science/article/pii/B9780128169452000080>
- [7] I. S. Khalil, A. Klingner, and S. Misra, Eds., *Chapter 7 - Principles of propulsion by magnetically actuated soft bodies: Magnetically actuated soft microrobots*. Academic Press, 2021. [Online]. Available: <https://www.sciencedirect.com/science/article/pii/B9780128169452000171>
- [8] L. SC, N.-V. S, and Z. M. Reese BE, "Unlocking the secrets of multi-flagellated propulsion: drawing insights from tritrichomonas foetus." *J R Soc Interface.*, 2014.



# Matlab Code

## A.1 Code for measuring Velocity

```
video=VideoReader('CellWith3Tails2.mp4')
%%
%Cell with 2 tails 1Hz
AantalFrames=8*45;
image(read(video,1*45));
[xbegin,ybegin]=ginput(2);
image(read(video,9*45));
[xeind,yeind]=ginput(2);
Afstand1=pdist([0,ybegin(1);0,yeind(1)]);
Afstand2=pdist([0,ybegin(2);0,yeind(2)]);

TotaleAfstand=mean([Afstand1,Afstand2]);
SnelheidPx1Hz3Tails=TotaleAfstand/(AantalFrames/45)
%%
%Cell with 2 tails 1,5Hz
AantalFrames=9*45;
image(read(video,12*45));
[xbegin,ybegin]=ginput(2);
image(read(video,21*45));
[xeind,yeind]=ginput(2);
Afstand1=pdist([0,ybegin(1);0,yeind(1)]);
Afstand2=pdist([0,ybegin(2);0,yeind(2)]);

TotaleAfstand=mean([Afstand1,Afstand2]);
SnelheidPx15Hz3Tails=TotaleAfstand/(AantalFrames/45)
%%
```

```

%Cell with 2 tails 2Hz
AantalFrames=11*45;
image(read(video,27*45));
[xbegin,ybegin]=ginput(2);
image(read(video,38*45));
[xeind,yeind]=ginput(2);
Afstand1=pdist([0,ybegin(1);0,yeind(1)]);
Afstand2=pdist([0,ybegin(2);0,yeind(2)]);

TotaleAfstand=mean([Afstand1,Afstand2]);
SnelheidPx2Hz3Tails=TotaleAfstand/(AantalFrames/45)
%%
%Cell with 2 tails 2,5Hz
AantalFrames=7*45;
image(read(video,42*45));
[xbegin,ybegin]=ginput(2);
image(read(video,49*45));
[xeind,yeind]=ginput(2);
Afstand1=pdist([0,ybegin(1);0,yeind(1)]);
Afstand2=pdist([0,ybegin(2);0,yeind(2)]);

TotaleAfstand=mean([Afstand1,Afstand2]);
SnelheidPx25Hz3Tails=TotaleAfstand/(AantalFrames/45)
%%
%Cell with 2 tails 3Hz
AantalFrames=12*45;
image(read(video,119*45));
[xbegin,ybegin]=ginput(2);
image(read(video,131*45));
[xeind,yeind]=ginput(2);
Afstand1=pdist([0,ybegin(1);0,yeind(1)]);
Afstand2=pdist([0,ybegin(2);0,yeind(2)]);

TotaleAfstand=mean([Afstand1,Afstand2]);
SnelheidPx3Hz3Tails=TotaleAfstand/(AantalFrames/45)
%%
%Cell with 2 tails 3,5Hz
AantalFrames=9*45;
image(read(video,136*45));

```



```

[xbegin,ybegin]=ginput(2);
image(read(video,145*45));
[xeind,yeind]=ginput(2);
Afstand1=pdist([0,ybegin(1);0,yeind(1)]);
Afstand2=pdist([0,ybegin(2);0,yeind(2)]);

TotaleAfstand=mean([Afstand1,Afstand2]);
SnelheidPx35Hz3Tails=TotaleAfstand/(AantalFrames/45)
%%
%Cell with 2 tails 4Hz
AantalFrames=7*45;
image(read(video,182*45));
[xbegin,ybegin]=ginput(2);
image(read(video,187*45));
[xeind,yeind]=ginput(2);
Afstand1=pdist([0,ybegin(1);0,yeind(1)]);
Afstand2=pdist([0,ybegin(2);0,yeind(2)]);

TotaleAfstand=mean([Afstand1,Afstand2]);
SnelheidPx4Hz3Tails=TotaleAfstand/(AantalFrames/45)
%%
%Cell with 2 tails 4,5Hz
AantalFrames=6*45;
image(read(video,196*45));
[xbegin,ybegin]=ginput(2);
image(read(video,202*45));
[xeind,yeind]=ginput(2);
Afstand1=pdist([0,ybegin(1);0,yeind(1)]);
Afstand2=pdist([0,ybegin(2);0,yeind(2)]);

TotaleAfstand=mean([Afstand1,Afstand2]);
SnelheidPx45Hz3Tails=TotaleAfstand/(AantalFrames/45)
%%
%Cell with 2 tails 5Hz
AantalFrames=11*45;
image(read(video,206*45));
[xbegin,ybegin]=ginput(2);
image(read(video,217*45));
[xeind,yeind]=ginput(2);

```

```

Afstand1=pdist([0,ybegin(1);0,yeind(1)]);
Afstand2=pdist([0,ybegin(2);0,yeind(2)]);

TotaleAfstand=mean([Afstand1,Afstand2]);
SnelheidPx5Hz3Tails=TotaleAfstand/(AantalFrames/45)

```

## A.2 Code for creating wave-functions and thrust force

```

%clear;close all;
t(1)=10;
fig = openfig('frame1tails10.fig');
axObjs = fig.Children;
dataObjs = axObjs.Children;
MatrixA(:,1) = dataObjs(1).XData;
MatrixA(:,2) = dataObjs(1).YData;
MatrixB=sortrows(MatrixA);
x(1,:)=MatrixB(:,1);
y(1,:)=MatrixB(:,2);

t(2)=20;
fig = openfig('frame1tails20.fig');
axObjs = fig.Children;
dataObjs = axObjs.Children;
MatrixA(:,1) = dataObjs(1).XData;
MatrixA(:,2) = dataObjs(1).YData;
MatrixB=sortrows(MatrixA);
x(2,:)=MatrixB(:,1);
y(2,:)=MatrixB(:,2);

t(3)=30;
fig = openfig('frame1tails30.fig');
axObjs = fig.Children;
dataObjs = axObjs.Children;
MatrixA(:,1) = dataObjs(1).XData;
MatrixA(:,2) = dataObjs(1).YData;
MatrixB=sortrows(MatrixA);
x(3,:)=MatrixB(:,1);
y(3,:)=MatrixB(:,2);

```

```

t(4)=40;
fig = openfig('frame1tails40.fig');
axObjs = fig.Children;
dataObjs = axObjs.Children;
MatrixA(:,1) = dataObjs(1).XData;
MatrixA(:,2) = dataObjs(1).YData;
MatrixB=sortrows(MatrixA);
x(4,:)=MatrixB(:,1);
y(4,:)=MatrixB(:,2);

Nim=30;xr=x;yr=y;clear x;clear y;t=t/45;f=1;T=1/f;
figure(2);
for i=1:Nim
    x(i,:)=max(xr(i,:))-xr(i,:);%move the sperm head to the origin and tail in pos
    y(i,:)=yr(i,:)-yr(i,length(yr(i,:)));
    p(i,2:5) = polyfit(x(i,:),y(i,:),3);
    yfit(i,:)=p(i,5)+p(i,4)*x(i,:)+p(i,3)*x(i,:).^2+p(i,2)*x(i,:).^3;
    l(i)=sum(((x(i,2:length(yfit(i,:)))-x(i,1:length(yfit(i,:)))-1)).^2+(y(i,2:length(yfit(i,:)))-yfit(i,2:length(yfit(i,:))))).^2);
    lfit(i)=sum(((x(i,2:length(yfit(i,:)))-x(i,1:length(yfit(i,:)))-1)).^2+(yfit(i,2:length(yfit(i,:)))-yfit(i,2:length(yfit(i,:))))).^2);
    %plot(x(i,:),y(i,:));
    hold on;xlabel('x [Pixel]');ylabel('y [Pixel]');
    plot(x(i,:),yfit(i,:));%pause(1);
end;

figure(2);
figure(3);plot(l);hold on;plot(lfit);xlabel('Image');ylabel('length [Pixel]');
legend('length from fit from image','length from polynomial function fit');
lavg=sum(l)/length(l);
lavgfit=sum(lfit)/length(l);

disp(['The average length is ',num2str(lavg),' (data) and ',num2str(lavgfit),' for

Ndx=200;Ns=20;
for i=1:Nim %for each image
    xs(i,1:Ndx)=(1:Ndx)*max(x(i,:))/Ndx; %intermediate points fine
    xs2(i,1:Ns)=(1:Ns)*max(x(i,:))/Ndx; %intermediate points rough

    phifits(i,:)=atan(p(i,4)+2*p(i,3)*xs(i,:)+3*p(i,2)*xs(i,:).^2); %slope of fitt
    for ix=1:Ndx

```

```

        ls(i,ix)=max(x(i,:))/Ndx*sum(cos(phifits(i,1:ix)).^(-1));%get the length for each
    end;
    for is=1:Ns
        k1=find(abs(ls(i,:)-max(ls(i,:))/Ns*is)==min(abs(ls(i,:)-max(ls(i,:))/Ns*is)));
        xs2(i,is)=xs(i,k1);
        ls2(i,is)=ls(i,k1);
        phifits2(i,is)=atan(p(i,4)+2*p(i,3)*xs2(i,is)+3*p(i,2)*xs2(i,is).^2);
    end;
    figure(4);plot(xs(i,:)',(phifits(i,:)-phifits(i,1)))';hold on;plot(xs2(i,:)',(phifits2(i,:)-phifits2(i,1)))';
    xlabel('x [Pixel]');ylabel('phi [Pixel]');title('Connection between x and phi');
    figure(8);hold off;plot(xs',ls');hold on;plot(xs2(1:i,:)','ls2(1:i,:)','o');
    xlabel('x [Pixel]');ylabel('length [Pixel]');title('Connection between x and length');
end;

% figure(5);polarplot(t/T*2*pi,phifittest);
% figure(6);plot(t/T*2*pi,phifittest);
% figure(8);plot(xs(1:9,:)-xL(1:9)-dx(1:9),ls(1:9,:));

for is=1:Ns
    phi0(is)=sum(phifits2(:,is)-phifits(:,1))/Nim;%first angle is subtracted to make s
end;
figure(11);hold off;plot(ls2(1,:)/max(ls(1,:)),phi0,'o-');%hold on;plot(ls2(2,:)/max(ls(2,:)),phi0,'o-');
xlabel('s/L');ylabel('\psi_0');

A=1;B=0.5;AB=[A,B];
for is=1:Ns
    [AB,ch2]=fminsearch(@psifit,AB,[],phifits2(:,is)-phifits(:,1)-phi0(is),t,f)
    A(is)=AB(1);
    B(is)=AB(2);
    figure(12);hold off;plot(t*1e3,phifits2(:,is)-phifits(:,1),'.-');hold on;plot(t*1e3,phifittest,'.-');
    xlabel('time [ms]');ylabel('\psi(s,t)-\psi_0(s)');legend('Data from Experiment','Best fit');
    pause(0.1);
end;
figure(13);plot(ls2(1,:)/max(ls(1,:)),(A.^2+B.^2).^0.5,'.-');
xlabel('s/L');ylabel('A=|\psi_1|=sqrt(A_1^2+A_2^2)');

figure(14);plot(ls2(1,:)/max(ls(1,:)), -atan2(A,B),'.-');
xlabel('s/L');ylabel('\phi=-arg(\psi_1)=-atan2(A,B)');
%%

```

```

for k=1:29
for i=0:38
dydx(i+1)=abs((yfit(k,end-1-i)-yfit(k,end-i))/(x(k,end-1-i)-x(k,end-i)));
if (isnan(dydx(i+1))) && (i>0)
    dydx(i+1)=dydx(i);
elseif isnan(dydx(i+1))
    dydx(i+1)=abs((yfit(k,end-2-i)-yfit(k,end-i))/(x(k,end-2-i)-x(k,end-i)));
end
dydt(i+1)=abs(((yfit(k,end-i)-yfit(k+1,end-i))/(10/45)));
normaldrag=4*pi/(log(70/5)+0.193);
parraleldrag=normaldrag/2;
Propforce(i+1)=(normaldrag-parraleldrag)*dydx(i+1)*dydt(i+1);
end
plot(Propforce)
AvgPropforce(1,k)=mean(Propforce);
end

%%
t=[0:10/45:280/45];
plot(t,AvgPropforce(1,:))
hold on
%plot(t,AvgPropforce(2,:))
%plot(t,AvgPropforce(3,:))
ylabel('Nondimensional F')
xlabel('Time (s)')
title('Average propulsive Force per tail over time')

```